J Solid State Electrochem (2012) 16:1537–1543
DOI 10.1007/s10008-011-1555-9

ORIGINAL PAPER

Mechanism studies and electrochemical performance optimization on $xLiFePO_4 \cdot (1-x)Li_3V_2(PO_4)_3$ hybrid materials

Hong Tang · Xiao-Dong Guo · Ben-He Zhong · Heng Liu · Yan Tang · Rui Xu · Long-Yan Li

Received: 19 July 2011 / Revised: 6 September 2011 / Accepted: 9 September 2011 / Published online: 4 October 2011
© Springer-Verlag 2011

Abstract Hybrid materials $xLiFePO_4 \cdot (1-x)Li_3V_2(PO_4)_3$ were synthesized by sol–gel method, with phenolic resin as carbon source and chelating agent, methylglycol as surfactant. The crystal structure, morphology and electrochemical performance of the prepared samples were investigated by X-ray diffraction (XRD), scanning electron microscopy (SEM), cyclic voltammetry (CV), galvanostatic charge–discharge test and particle size analysis. The results show that $LiFePO_4$ and $Li_3V_2(PO_4)_3$ co-exist in hybrid materials, but react in single phase. Compared with individual $LiFePO_4$ and $Li_3V_2(PO_4)_3$ samples, hybrid materials have smaller particle size and more uniform grain distribution. This structure can facilitate Li ions extraction and insertion, which greatly improves the electrochemical properties. The sample $0.7LiFePO_4 \cdot 0.3Li_3V_2(PO_4)_3$ retains the advantages of $LiFePO_4$ and $Li_3V_2(PO_4)_3$, obtaining an initial discharge capacity of 166 mA h/g at 0.1 C rate and 109 mA h/g at 20 C rate, with a capacity retention rate of 73.3% and an excellent cycle stability.

Keywords Hybrid materials · $LiFePO_4$ · $Li_3V_2(PO_4)_3$ · Phenolic resin · Sol–gel method

Introduction

Since Padhi et al. [1] first reported that $LiFePO_4$ could insert and extract Li ions reversibly, $LiFePO_4$ has been considered as one having the most potential and the most challenged cathode materials. After more than 10 years' development, the bottleneck for $LiFePO_4$ commercial application-poor conductivity, resulting from the low lithium-ion diffusion rate and low electronic conductivity, has been settled by doping metal ions or carbon coating [2–5]. However, in order to apply it in hybrid electrical vehicles (HEV), the current major issue needed to be resolved is how to improve its discharge capacity and poor cycle stability at high discharge rate. On the other hand, $Li_3V_2(PO_4)_3$, which was reported almost at the same time, has a large theoretical specific capacity and excellent cycle stability, thereby drawing much attention [6, 7]. In recent years, a lot of progress has been made concerning $Li_3V_2(PO_4)_3$ as cathode materials [8–11], in terms of its complicated internal reaction mechanism and structural transformation under different charging and discharging voltages [12]; the industrial development of $Li_3V_2(PO_4)_3$ has not been reported yet, just staying on the stage of experimental research.

Our group has found that the specific capacity of $LiFePO_4$ is high at low rate, but attenuates seriously at high rate, exhibiting poor rate performance [13], which limits its application in large electrical powers. From this point of view, $Li_3V_2(PO_4)_3$ shows an opposite trend to that of $LiFePO_4$ [14]. Since their structures and preparation methods are similar, we can therefore imagine preparing hybrid materials by mixing $LiFePO_4$ and $Li_3V_2(PO_4)_3$ at a certain ratio, which can meet the requirements of high-energy power batteries. Yang et al. [15] synthesized well-crystallized $LiFePO_4$-based powders with V addition substituting for Fe, which exhibited a high discharge capacity of about 100 mA h/g at 10 C. Hu et al. [16] also studied V-doping for $LiFePO_4$-based Li ion batteries, and their results indicated that V ions were doped in $LiFePO_4$ and did not alter its crystal structure. Zheng et al. [17–20] synthesized

H. Tang · X.-D. Guo · B.-H. Zhong (✉) · H. Liu · Y. Tang · R. Xu · L.-Y. Li
Phosphorus Resource Utilization Center of Chinese Ministry of Education, College of Chemical, Engineering, Sichuan University, Chengdu 610065, China
e-mail: zhongbenhe@hotmail.com

$x LiFePO_4 \cdot y Li_3V_2(PO_4)_3$ using wet chemical reduction at room temperature, replacing part of $LiFePO_4$ by $Li_3V_2(PO_4)_3$ with higher ionic conductivity to improve the ionic conductivity of composite materials, whose overall performance has improved greatly. Xiang et al. [21] also prepared $9LiFePO_4 \cdot Li_3V_2(PO_4)_3/C$ via carbon thermal reduction method, which showed good rate performance and cycle stability whether at low or high discharge rate. All these results indicate that $LiFePO_4$ and $Li_3V_2(PO_4)_3$ have good compatibility, so preparing the hybrid materials via optimization method is viable.

In this paper, a series of hybrid materials were synthesized by sol–gel method, which ensures a potentially higher purity and homogeneity than traditional solid-state reaction method used by other researchers. The authors have found on the way that different ratios of $LiFePO_4$ and $Li_3V_2(PO_4)_3$ affected the properties of the materials under the same preparation conditions, just changing the ratios of the two materials. In the preparation process, using cheaper $FePO_4 \cdot 2H_2O$ as raw materials in comparison with $FeC_2O_4 \cdot 2H_2O$ can reduce the cost greatly. Phenolic resin was used as carbon source and chelating agent, which would decompose into elemental carbon in the calcination process. The residual carbon not only serves as a reduction agent, but can also act as a conductive agent to solve the low-conductivity problem that $LiFePO_4$ and $Li_3V_2(PO_4)_3$ both have.

Experimental

Materials and preparation

$LiOH \cdot H_2O$ (99%), $FePO_4 \cdot 2H_2O$ (98.5%), LiH_2PO_4 (99.5%) and NH_4VO_3 (99.5%) were weighed in accordance with $x LiFePO_4 \cdot (1-x) Li_3V_2(PO_4)_3$ (x=0, 0.3, 0.5, 0.7 and 1), using water bath to keep the temperature of reaction system at 80°C. The weighed $LiOH \cdot H_2O$ and LiH_2PO_4 were dissolved in distilled water, then placed into a flask, with constant stirring. After adding about 10 ml methylglycol as surfactant, NH_4VO_3 and $FePO_4 \cdot 2H_2O$ were added in turn; next, red solution was obtained after stirring for 1 h, dropping 15 ml phenolic resin dissolved in ethanol at 2 drops/s. The mixture would turn into blue-black sol, which turned into gel through vacuum distillation, dried at 90°C for 10 h in a drying oven. The reaction equations were as follows:

$$LiOH + FePO_4 + [C_8H_8O_2]_n \rightarrow LiFePO_4/C + CO + H_2O + CO_2$$

$$LiH_2PO_4 + NH_4VO_3 + [C_8H_8O_2]_n \rightarrow Li_3V_2(PO_4)_3/C + NH_3 + CO + H_2O + CO_2$$

Precursor powder was calcined in tube furnace under nitrogen atmosphere, maintained at 700°C for 12 h. The prepared materials were denoted as samples A, B, C, D and E (x=0, 0.3, 0.5, 0.7 and 1, respectively) according to different x values.

Characterization

The crystalline structure of each product was analyzed by X-ray diffraction (XRD; D/max-rB, Rigaku, Cu Kα radiation) (λ=1.5046 Å) operated at 40 kV and 40 mA. The particle morphology and particle size of the samples were observed by scanning electron microscopy (SEM; SPA400 Seiko Instruments). The particle size distribution was tested by laser particle size distribution tester (JL-6000). The analytical instrument (CS-902, Wanlianda Xinke, Beijing, China) was employed to test the carbon content. The cyclic voltammetry (CV) tests were performed on a CHI660B electrochemical workstation.

Battery preparation and measurement

The electrochemical performance of the synthesized materials was tested by galvanostatic charge–discharge method. Metal lithium foils were used as the counter-electrodes. The working cathode was composed of 80 wt.% hybrid materials, 13 wt.% acetylene black as conducting agent and 7 wt.% polyvinylidene fluoride (PVDF) as binder. After being blended in *N*-methylpyrrolidinone (NMP), the mixtures were spread uniformly onto a thin Al foil, and its surface must be cleaned from oxide layer before coating with electrode materials, dried in vacuum at 120°C for 15 h and then cut into pieces with diameter of 1.4 cm; thus, the area of the active electrode surface was 1.5386 cm^2. The electrolyte was 1 M $LiPF_6$ solution in a mixed solvent of ethylenecarbonate (EC) and dimethyl carbonate (DMC) (EC/DMC=1:1, v/v), celgard2400 as the separator. The coin type cells were assembled in an argon-filled glove box. The cells were galvanostatically charged and discharged at room temperature between 2.5 and 4.5 V versus Li^+/Li on the electrochemical test instrument.

Results and discussion

Effect of mixing ratios on the properties of the samples

Figure 1 illustrates the XRD patterns of the samples; the sharp peaks in the patterns indicate that all samples are well crystallized. As can be observed in the figure, when x=0 and 1, the synthesized materials are $Li_3V_2(PO_4)_3$ with an ordered monoclinic structure and $LiFePO_4$ with olivine structure, respectively, with no impurities phase detected. When x=0.3, 0.5 and 0.7, the characteristic peaks of $LiFePO_4$ and $Li_3V_2(PO_4)_3$ both appear in the XRD patterns, with the ratios of the two materials changing, and there is

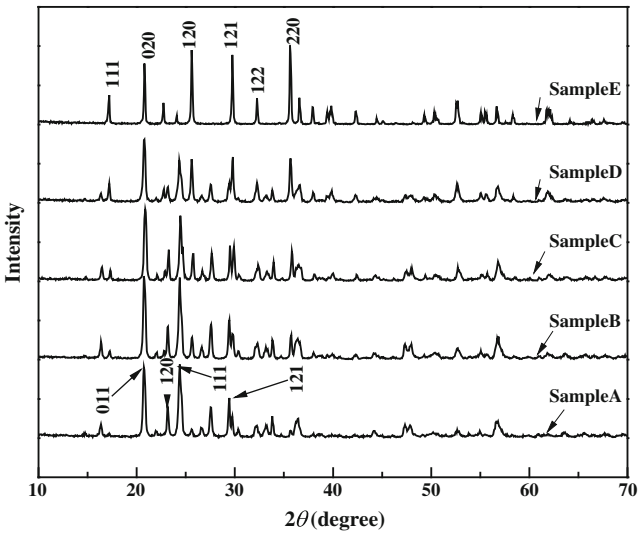

Fig. 1 XRD patterns of the samples

considerable difference in the characteristic peaks. As the content of $LiFePO_4$ increases, the characteristic peak intensity of $Li_3V_2(PO_4)_3$ gradually reduces and finally disappears, as that of $LiFePO_4$ starts to appear and becomes stronger. This phenomenon demonstrates that hybrid materials consist of the two materials. In order to set forth the effect of adding part of $Li_3V_2(PO_4)_3$ to $LiFePO_4$, we have calculated all the samples' unit cell lattice parameters based on JCPDS 83–2092 of $LiFePO_4$ (see Table 1). The crystallinity of all samples synthesized by sol–gel method reaches to 95% (calculated via Jade software), which shows that all samples crystallize well through the above preparation process. *B* and *c* values have different degrees of increase with *a* value decreasing, which was attributed to that $Li_3V_2(PO_4)_3$ existing in hybrid materials extrudes $LiFePO_4$ cell; the extrusion force causes the change in unit cell parameters. Meanwhile, all cell volumes (based on the pure $LiFePO_4$ volume) decrease, so the diffusion pathway of Li ions becomes shorter to facilitate them inserting and extracting. This structure can significantly contribute to the electrochemical performances of the materials. We know that carbon coating on the particle surface is very important for cathode materials, which can prevent particles from aggregating and increase the electrical conductivity of the samples [4, 5]. However, there is no evidence of carbon in XRD patterns because of its amorphous state. Thus we have tested all these samples' carbon contents (see Table 1), which are all about 2.5% with no big difference. Accordingly we can affirm that their electrochemical performance differences are not due to the carbon content, but to the different ratios of $LiFePO_4$ and $Li_3V_2(PO_4)_3$.

The specific capacities of as-prepared samples at different discharge rates are listed in Table 2, which were tested at various C rates from 0.1 C to 20 C (1 C=170 mA/g). It can be clearly seen that $LiFePO_4$ is strongly affected by the C rate, its specific capacity is high at low discharge rate, up to 146 mA h/g at 0.1 C, which decreases quickly at high rate, only remaining 77 and 67 mA h/g at 10 C and 20 C, respectively. Compared to $LiFePO_4$, the property of $Li_3V_2(PO_4)_3$ differs little from low rate to high; its specific capacity is only 129 mA h/g at 0.1 C, which has a small amount of fading with discharge rate is increased, keeping 110 and 97 mA h/g at 10 C and 20 C, respectively. Furthermore, all hybrid materials exhibit higher specific capacities than the individual $LiFePO_4$ and $Li_3V_2(PO_4)_3$ under all current densities tested. Among them, the discharge capacity of sample D ($0.7LiFePO_4 \cdot 0.3Li_3V_2(PO_4)_3$) is the highest, which is up to 166 mA h/g at 0.1 C, achieving 109 mA h/g at 20 C, with a retention rate of 73.3%. The results are much better than what other investigators have reported [17, 21]. In this case, we can consider scale-up experiments.

Figure 2 shows the rate performance of the samples at different discharge rates. $Li_3V_2(PO_4)_3$ (sample A) exhibits good rate performance both at low discharge rate of 0.1 C and high rate of 20 C, and the specific capacities attenuate little at the same discharge rate. However, the rate performance of $LiFePO_4$ is much worse than that of $Li_3V_2(PO_4)_3$, including larger capacity attenuation and poorer cyclic stability. However, the performances of all hybrid materials are improved to some extent by mixing the two materials, and sample D has the best cycle stability and rate performance. To further observe the cyclic performance of sample D at high discharge rate, the cell was cycled for 1,000 times at 10 C discharge rate. After testing at 20 C, the

Table 1 Unit cell parameters and carbon contents of the samples

Samples	Crystallinity (%)	Average grain size (nm)	*a* (nm)	*b* (nm)	*c* (nm)	*V* (nm^3)	Carbon content (%)
A (*x*=0)	95.10	3.702	–	–	–	–	2.550
B (*x*=0.3)	94.29	2.99	1.028323	0.60028	0.46890	0.2883	2.612
C (*x*=0.5)	94.66	2.83	1.030277	0.60088	0.47099	0.2893	2.585
D (*x*=0.7)	95.25	2.52	1.028773	0.60000	0.46985	0.2899	2.498
E (*x*=1)	95.51	1.374	1.031777	0.60000	0.46870	0.2901	2.503
Standard $LiFePO_4$	–	–	1.0334	0.6008	0.4693	0.291392	–

Table 2 Specific capacities of the samples at different discharge rates

Samples	0.1 C	0.2 C	0.5 C	1 C	3 C	5 C	10 C	20 C
A (x=0)	129	126	122	119	115	112	110	97
B (x=0.3)	134	130	126	122	115	110	105	95
C (x=0.5)	139	136	132	129	125	122	116	96
D (x=0.7)	166	162	156	152	143	137	127	109
E (x=1)	146	138	133	126	103	88	77	67

results shown in Fig. 3 indicate that sample D exhibits an excellent cyclic performance; there is less than 1% discharge capacity loss over 1,000 times at 10 C.

The good cyclic stability and low attenuation of $Li_3V_2(PO_4)_3$ have a great relationship with its crystal structure. There are two major crystal structures about $Li_3V_2(PO_4)_3$, diamond and monoclinic (we mainly focus on the latter). When the charge voltage is set between 2.5 and 4.5 V, only two Li ions will extract and insert; another one can support the frame, so that its structure cannot be destroyed as the discharge rate is increased, and its volume changes little during phase transformation. By XRD analysis, the monoclinic structure can be restored after being discharged, so it has better reversibility and higher discharge capacity even at 20 C. For $LiFePO_4$, once the charge–discharge process begins, it will generate a $Li_xFePO_4/Li_{1-x}FePO_4$ two-phase interface, and the interface area shrinks gradually along with Li ions' extracting and inserting. When it reaches the critical surface area, the migration of interface can no longer support the high current, so that the electrochemical action will be under diffusion control [1]. After Li ions' extraction, both the electronic and ion conductivities of generated $FePO_4$ are low; therefore, it is not conductive to conducting, resulting in poor electrochemical performance. Above all, since $LiFePO_4$ and $Li_3V_2(PO_4)_3$ exist in a separate phase in the hybrid materials, the hybrid materials can combine the advantages of the two materials well, thereby achieving good properties.

Reasons for the excellent performance of sample D

Figure 4 shows the charge–discharge curves of samples A, D and E at 0.1 C and 20 C, respectively. Sample A ($Li_3V_2(PO_4)_3$) has three charge–discharge plateaus at 0.1 C, although not very obvious, indicating whose charge–discharge processes are multi-phase reaction process; only two plateaus can be seen at 20 C with the third one vanishing. For sample E ($LiFePO_4$), only one stable plateau can be seen at 3.44 V, and the interval between charge and discharge plateau is small at 0.1 C. This interval becomes much bigger at 20 C and the plateaus almost disappear, showing a large polarization. This also explains why the specific capacity of $LiFePO_4$ fades quickly at high discharge rate. Sample D ($0.7LiFePO_4{\cdot}0.3Li_3V_2(PO_4)_3$) has four plateaus, all of which are stable at 0.1 C. The interval between charge and discharge curves is much smaller than those of $LiFePO_4$ and $Li_3V_2(PO_4)_3$, indicating good electrochemical performances at low discharge rate. Even at 20 C the plateaus continue to exist, only less stable and showing a bigger interval.

Figure 5 shows the CV curves of samples A, D and E tested between 2.5 and 4.5 V at a scan rate of 0.1 mV/s. The first three CV curves overlap basically, implying that all three samples have perfect cyclic stability. There are three

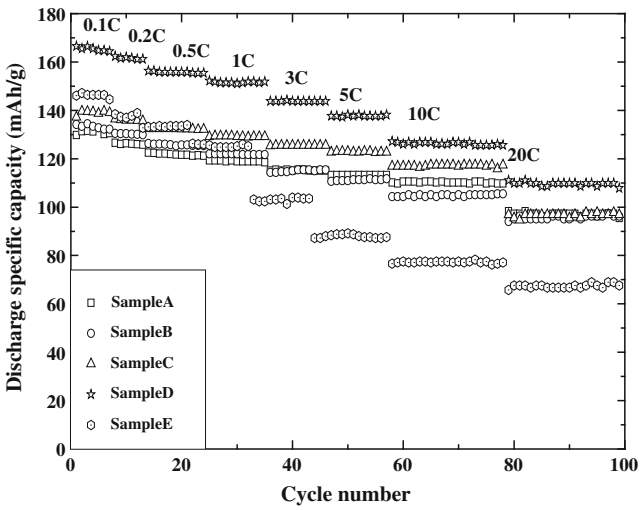

Fig. 2 Cycle performance of the samples at different discharge rates

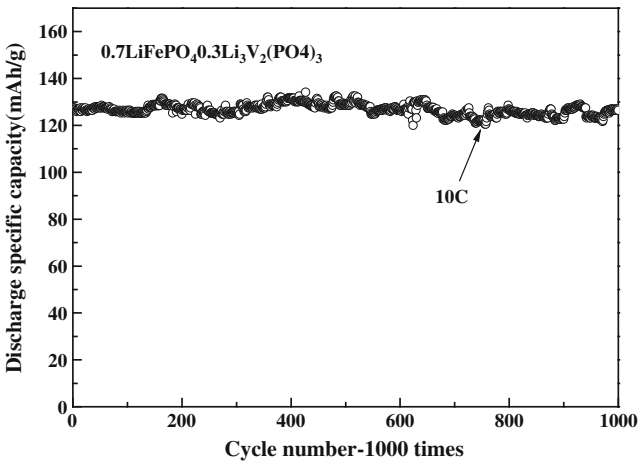

Fig. 3 The cyclic performance of sample D at 10 C

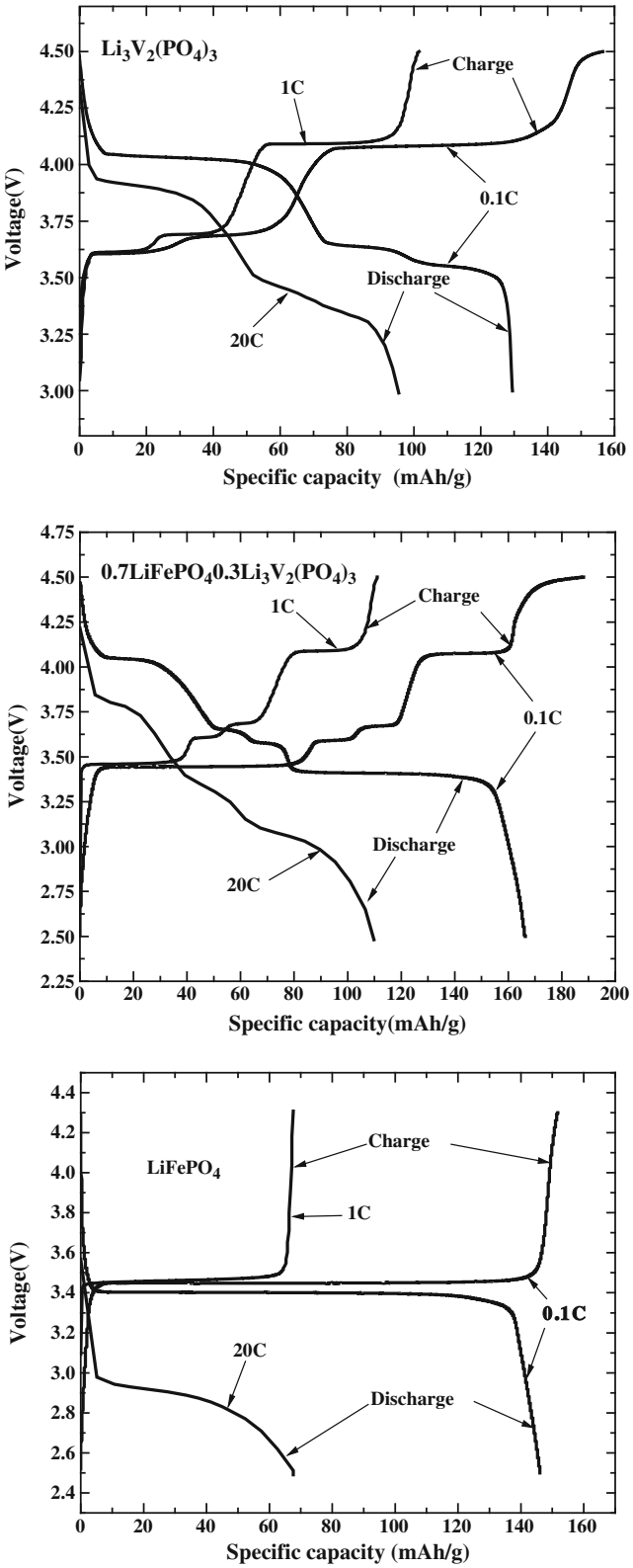

Fig. 4 Charge–discharge curves of samples A, D and E

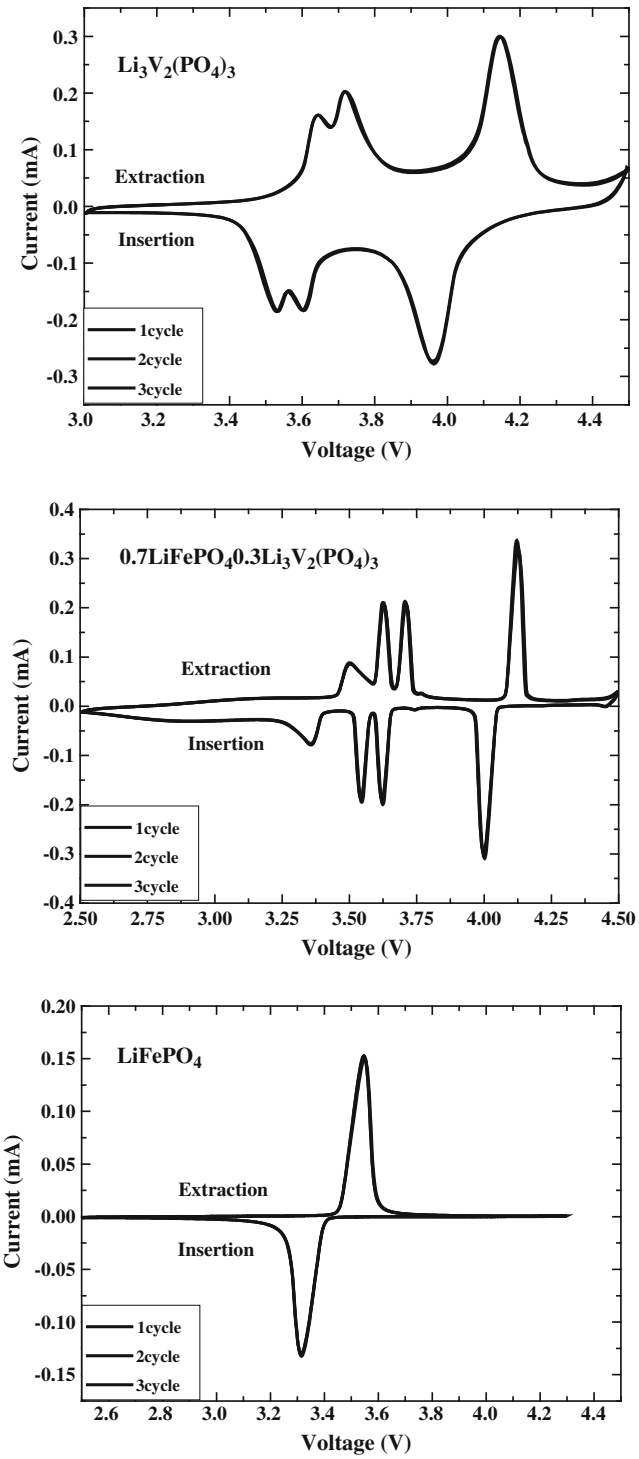

Fig. 5 CV curves of samples A, D and E

pairs of redox peaks in the CV curves of sample A ($Li_3V_2(PO_4)_3$), located at (3.625 V, 3.55 V), (3.75 V, 3.625 V) and (4.125 V, 3.975 V), corresponding to the complex phase changes between following single-phase, $Li_3V_2(PO_4)_3 \rightarrow Li_{2.5}V_2(PO_4)_3$, $Li_{2.5}V_2(PO_4)_3 \rightarrow Li_2V_2(PO_4)_3$, $Li_2V_2(PO_4)_3 \rightarrow Li_1V_2(PO_4)_3$, respectively. Only one pair of redox peaks appears in the CV curves of sample E ($LiFePO_4$), corresponding to a two-phase reaction between lithiated phase $LiFePO_4$ and

delithiated phase $FePO_4$. There are four pairs of redox peaks in the CV curves of sample D ($0.7LiFePO_4 \cdot 0.3Li_3V_2(PO_4)_3$), which consist of both the redox peaks of $LiFePO_4$ and $Li_3V_2(PO_4)_3$. Either from the peak position or the numbers of the peaks, we confirm that the hybrid materials are made up of the two cathode materials, which maintain their original feathers. On the whole, the CV curves are completely consistent with the charge–discharge curves.

SEM images of samples A, D and E are shown in Fig. 6. Sample A ($Li_3V_2(PO_4)_3$) has a non-uniform particle size distribution, with large-size particles. Although there are no large particles in sample E ($LiFePO_4$), it still has the

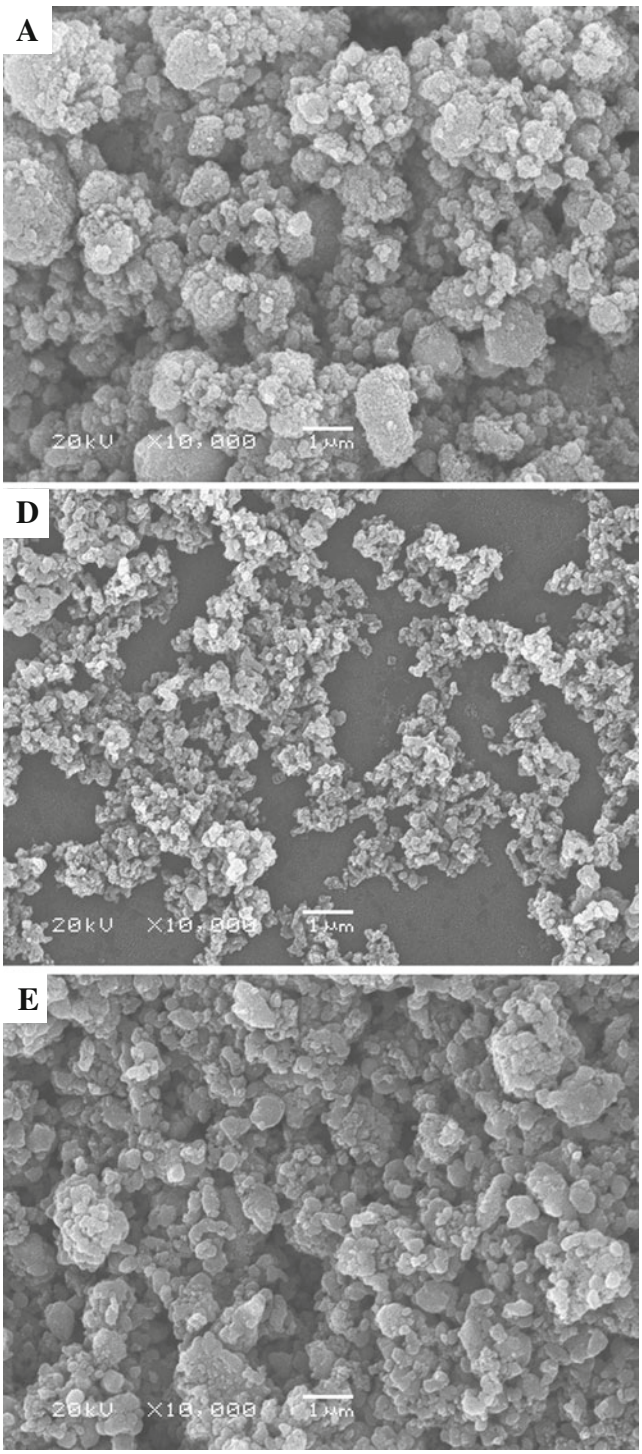

Fig. 6 SEM images of samples A, D and E

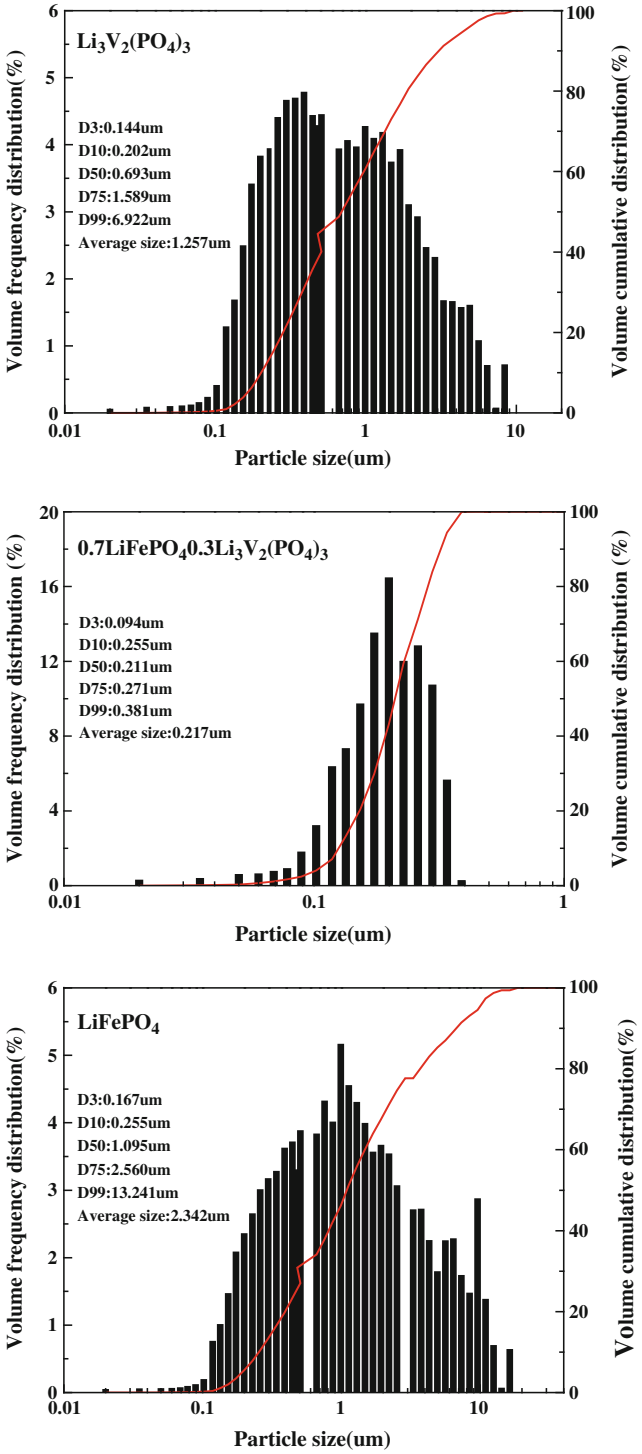

Fig. 7 Particle size distribution of samples A, D and E

phenomena of uneven particle size distribution and serious agglomeration. Sample D ($0.7LiFePO_4 \cdot 0.3Li_3V_2(PO_4)_3$) has an average grain size in the range of 50–100 nm, with uniform particle size distribution and no obvious aggregation, because $LiFePO_4$ and $Li_3V_2(PO_4)_3$ exist separately in hybrid material, and the surface energy of the particle surface is different because of the different structures, which to some extent plays a role in prevention of particle agglomeration. The corresponding particle size distributions of the samples are shown in Fig. 7 (tested by JL-6000 laser particle size distribution tester), which are consistent with SEM images, but larger than the values reflected by the SEM images, because of minor reunion. In connection with the electrochemical performance of the samples, we conclude that particle size has a great effect on the performance of the samples: the smaller the better, especially the specific capacity and cyclic stability of high discharge rates. This is because the solid-state diffusion distance of Li ions is shorter in small internal particles; thus, the diffusion rate is able to maintain high current needs even when the discharge rate is increased to 20 C, so that the material shows good rate capability.

Conclusions

Hybrid materials were synthesized by sol–gel method, and XRD, SEM, CV and constant current test were used to investigate the morphology and performance of the samples. The results showed $LiFePO_4$ and $Li_3V_2(PO_4)_3$ existed in their own structures in hybrid materials, thus they are not affected by others. The performance of sample $0.7LiFePO_4 \cdot 0.3Li_3V_2(PO_4)_3$ was much better than the rest, with particle size in the range of 50–100 nm, achieving high specific capacity and excellent cyclic stability both at low and high discharge rate. Its initial discharge specific capacity reached 166 mA h/g at 0.1 C rate, remaining 127 mA h/g at 10 C and 109 mA h/g at 20 C. The results have significant meaning for industrialization of hybrid materials used as power source for electric cars.

Acknowledgements This work was funded by the National Scientific and Technical Backup Plan of China (No. 2007BAQ01055). The Analysis and Test Center, Polymer Engineering National Key Laboratory of Sichuan University also supported this study.

References

1. Padhi AK, Nanjundaswamy KS, Goodenough JB (1997) J Electrochem Soc 144:1188–1194
2. Li LJ, Li XH, Wang ZX, Guo HJ, Wu L, Hao Y, Zheng JC (2010) J Alloy Compd 497:176–181
3. Arumugam D, Paruthimal Kalaignan G, Manisankar P (2009) J Solid State Electrochem 13:301–307
4. Huang YH, Ren HB, Peng ZH, Zhou YH (2009) Electrochim Acta 55:311–315
5. Yao J, Konstantinov K, Wang GX, Liu HK (2007) J Solid State Electrochem 11:177–185
6. Wang L, Zhang LC, Lieberwirth Ingo, Xu HW, Chen CH (2010) Electrochem Commun 12:52–55
7. Qiao YQ, Wang XL, Zhou Y, Xiang JY, Zhang D, Shi SJ, Tu JP (2010) Electrochim Acta 55:510–516
8. Chen ZY, Dai CS, Wu G, Nelson M, Hu XG, Zhang RX, Liu JS, Xia JC (2010) Electrochim Acta 55:8595–8599
9. Rui XH, Li C, Liu J, Cheng T, Chen CH (2010) Electrochim Acta 55:6761–6767
10. Zhai J, Zhao MS, Wang DD, Qiao YQ (2010) J Alloy Compd 502:401–406
11. Zhang L, Wang XL, Xiang JY, Zhou Y, Shi SJ, Tu JP (2010) J Power Sources 195:5057–5061
12. Qiao YQ, Wang XL, Xiang JY, Zhang D, Liu WL, Tu JP (2011) Electrochim Acta 56:2269–2275
13. Tang Y, Guo XD, Zhong BH, Liu H (2010) Inor Chem Industry 6:12–14
14. Tang Y, Zhong BH, Guo XD, Liu H, Zhong YJ, Xiang N, Tang H (2011) Acta Phys-Chim Sin 27:869–874
15. Yang MR, Ke WH, Wu SH (2007) J Power Sources 165:646–650
16. Hu N, Wang CY, Kang XY, Wumair T, Han Y (2010) J Alloy Compd 503:204–208
17. Zheng JC, Li XH, Wang ZX, Li JH, Wu L, Li LJ, Guo HJ (2009) Acta Phys-Chim Sin 25:1916–1920
18. Zheng JC, Li XH, Wang ZX, Li JH, Li LJ, Wu L, Guo HJ (2009) Ionics 15:753–759
19. Zheng JC, Li XH, Wang ZX, Niu SS, Liu DR, Wu L, Li LJ, Li JH, Guo HJ (2010) J Power Sources 195:2935–2938
20. Zheng JC, Li XH, Wang ZX, Qin DM, Guo HJ, Peng WJ (2009) J Inorg Mater 24:143–146
21. Xiang JY, Tu JP, Zhang L, Wang XL, Zhou Y, Qiao YQ, Lu Y (2010) J Power Sources 195:8331–8335